

Tailoring MCM-41 Mesoporous Silica Particles through Modified Sol-Gel Process for Gas Separation

Open
Access

Wong Yean Sang^{1,*}, Oh Pei Ching¹

¹ Chemical Engineering Department, Universiti Teknologi PETRONAS, 32610 Seri Iskandar, Perak, Malaysia

ARTICLE INFO

ABSTRACT

Article history:

Received 2 December 2017

Received in revised form 30 January 2018

Accepted 10 February 2018

Available online 18 February 2018

Mobil Composition of Matter-41 (MCM-41) is recognized as a potential filler to enhance permeability of mixed matrix membrane (MMM). However, the required loading for available micron-sized MCM-41 was considerably high in order to achieve desired separation performance. In this work, reduced-size MCM-41 was synthesized to minimize filler loading, improve surface modification and enhance polymer-filler compatibility during membrane fabrication. The effect of reaction condition, stirring rate and type of post-synthesis washing solution used on particle diameter of resultant MCM-41 were investigated. It was found that MCM-41 produced at room temperature condition yielded particles with smaller diameter, higher specific surface area and enhanced mesopore structure. Increase of stirring rate up to 500 rpm during synthesis also reduced the particle diameter. In addition, replacing water with methanol as the post-synthesis washing solution to remove bromide ions from the precipitate was able to further reduce the particle size by inhibiting polycondensation reaction. It was also noticed that particle diameter of MCM-41 is optimized with 15 hours of calcination.

Keywords:

MCM-41, particle diameter, reaction parameter, separation

Copyright © 2018 PENERBIT AKADEMIA BARU - All rights reserved

1. Introduction

In the past decade, membrane technology has received significant attention in the industry as a promising separation technique for gas pairs due to several advantages such as high efficiency, ease of operation and low capital and operating costs [1]. Membrane-based gas separation are currently applied in processes including natural gas separation, hydrogen recovery and oxygen/nitrogen enrichment [2-4]. However, current polymeric membranes have reached the general trade-off between permeability and selectivity [5]. In order to outreach the upper bound limit of Robeson's curve, MMM was introduced. MMM consists of inorganic filler dispersed in polymer matrix. Inorganic particles are known to have high selectivity characteristic whereas polymeric membrane offers high permeability which eventually enhance the performance of membrane. In previous work, several types of inorganic materials were successfully incorporated into MMM for instance

* Corresponding author.

E-mail address: peiching.oh@utp.edu.my (Wong Yean Sang)

layered silicate [6], single walled carbon nanotube [7], zeolite [8], and silicate mesoporous materials [9]. Among them, MCM-41 (Mobil Composition of Matter-41), a type of mesoporous silica was often selected as filler due to high porosity which favors gas diffusion. It has a regular pore system that is well-arranged in hexagonal array with pore sizes ranging from 2 nm to 10 nm and narrow pore diameter distribution. This well-defined structure of MCM-41 is commonly produced from hexadecyltrimethylammonium bromide (CTAB, template) and tetraethylorthosilicate (TEOS, source of silica). Figure 1 displays the templating mechanism for MCM-41.

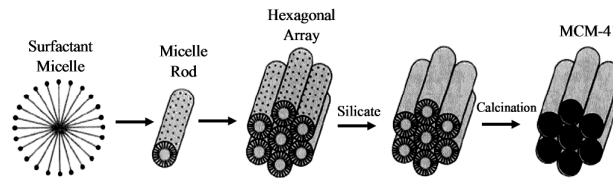
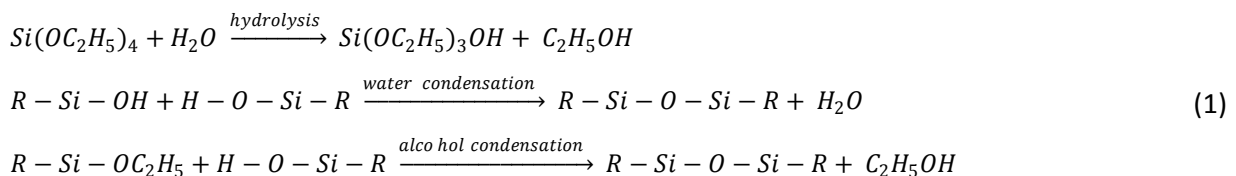


Fig. 1. Schematic model of templating mechanism for MCM-41 [12]

In order to prepare high quality MCM-41 in a short period of time, sol-gel process is often applied due to its ability to produce pure and homogeneous product at mild conditions [10]. Sol-gel process involves hydrolysis and condensation of metal alkoxide such as tetraethylorthosilicate (TEOS) in the presence of acid or base as the catalyst [11]. Equation (1) below outlined the general reactions of TEOS that lead to the formation of MCM-41 through sol-gel process.



Many studies demonstrated that incorporating MCM-41 into MMM leads to a substantial increase in permeability without sacrificing the selectivity [13-15]. MCM-41 also possesses high specific surface area (approximately between 700 m² g⁻¹ to 1500 m² g⁻¹) and high thermal stability which will help to strengthen the physical properties of membrane. However, in order to achieve this performance, loading of MCM-41 required was considerably high (up to 30 weight percent). It was postulated that reducing the particle diameter of MCM-41 will ultimately reduce the loading required, leading to a more economically viable alternative. This is because reduced-size MCM-41 shows enhancement in physical and chemical properties that will directly affect filler-polymer compatibility in MMM.

2. Previous Works

Throughout the years, numerous attempts have been done by researchers in order to produce small diameter, highly crystalline MCM-41 within short period of synthesis. In previous work by Grün and colleagues [16], highly ordered MCM-41 were successfully synthesized at room temperature followed by 10 days of aging at 378K and 5 hours of calcination at 823K. X-ray diffraction (XRD) pattern of this two-step-synthesized MCM-41 showed 3 sharp Bragg peaks at plane 100, 110, and 200 of the hexagonal system. However, the average particle diameter of

resultant MCM-41 was large, at approximately 1100 nm. Besides, the procedure involves a long synthesis duration. In a later study, Teymouri *et al.*, [17] tried to shorten the synthesis period and carried out only 5 hours of aging in the synthesis of MCM-41. A more defined and organized structure of small diameter MCM-41 (average diameter of 475 nm) was successfully formed with 4 sharp Bragg peaks at plane 100, 110, 200 and 210 before calcination. However, SEM image of the resultant sample after calcination showed particles with distorted spherical shape. It is hypothesized that with short hours of aging, covalent bond between silicates particles arranged in hexagonal array are relatively weak which lead to distorted spherical shape after removal of template. Recently, Melendez-Ortiz *et al.*, [18] prepared MCM-41 at different hydrothermal synthesis duration between 48 hours and 110 hours. In their research, it was found that longer reaction time results in higher order of MCM-41 structure. This was evident in the intense peak at XRD plane 100, 110 and 200. Nonetheless, pore size of the prepared MCM-41 is comparatively larger than existing literatures (by approximately 20%) [16, 17]. In another study by Kim and Marand [14], particles with average diameter of 80 nm were successfully formed by using sodium hydroxide as catalyst. But it was noticed that the resultant MCM-41 were in amorphous state with low crystallinity. This finding was supported by the broad and low intensity XRD Bragg peaks of as-synthesized MCM-41.

Although it is clear that the presence of charged surfactant in sol-gel process will eventually lead to the formation of MCM-41, reaction conditions and procedures that are able to produce the final product with reduced particle size and highly crystalline mesopore structure are still ambiguous. Hence, in this work, particle size of MCM-41 was tailored by varying the important preparation parameters such as reaction condition (room temperature vs hydrothermal), solution stirring rate, types of post-synthesis washing solution and period of calcination. The effects of preparation parameters toward particle size of MCM-41 were systematically studied with the intention to produce reduced diameter MCM-41 which favors MMM fabrication process and gas separation process.

3. Materials

Hexadecyltrimethylammonium bromide (CTAB for synthesis), tetraethylorthosilicate (TEOS for synthesis), ethanol (purity ≥ 99.5 wt%, analysis grade) and methanol (purity ≥ 99.8 wt%, analysis grade) were purchased from Merck Sdn Bhd. Ammonium hydroxide (NH₄OH, 35 wt% analytical reagent grade) was purchased from Fluka. All chemicals were used without further purification.

4. Synthesis Methods

A. Room Temperature (RT) Synthesis

Preparation method by Grün and colleagues [16] was adapted and modified. 2.5 g of CTAB (0.007 mol) was dissolved in a solution containing 50 ml of deionized water, 15 ml of ammonium hydroxide (0.25 mol) and 76 ml of ethanol (1.3 mol). The solution was stirred for 15 minutes at 250 rpm or 500 rpm. 5 ml of TEOS (0.023 mol) was added and stirred for 2 hours at the same rate resulting in a concentrated solution with white precipitate that has the following molar ratio 1 TEOS: 0.3 CTAB: 11 NH₄OH: 144 H₂O: 58 C₂H₅OH. The resultant white precipitate was filtered and washed with deionized water and methanol or with methanol only. The collected precipitate was dried in an oven for 12 hours at 363 K. The dried sample was calcined at 823 K in furnace and kept at this temperature for 5, 10, 15 or 20 hours.

B. Hydrothermal (HT) Synthesis

For hydrothermal synthesis, MCM-41 was prepared according to the aforementioned procedure and molar composition at room temperature. After stirring for 2 hours, the concentrated solution was transferred into a teflon-lined autoclave and aged for 3 days at 378 K. The solution was then filtered and washed. The collected precipitate was oven dried at 363 K and calcined at 823 K.

5. Characterization

Nitrogen adsorption and desorption of particles were measured on Micromeritics ASAP 2020 surface analyzer. Brunauer Emmett Teller (BET) method was used to calculate specific surface area of particles from adsorption isotherm. The samples were degassed at 423 K and 1 mPa for 12 hours before measurements were taken. Calcined MCM-41 sample was placed into sample holder through back loading method. XRD patterns were recorded on PANalytical X'Pert3 Powder using Cu K α radiation of wavelength 0.15405 nm. Diffraction data were recorded in the 2 θ range of 2° to 10° using a step size of 0.01° and exposure time of 200 s per step. Field emission electron microscopy (FESEM) images of samples coated with gold were also taken using Zeiss Supra55 VP. Average particles' diameter was measured on FESEM images.

5. Results and Discussion

A. Influence of Reaction Condition (Room Temperature vs Hydrothermal)

Table 1 shows the properties of MCM-41 synthesized via different reaction parameters. It was observed that MCM-41 prepared under room temperature condition (sample T2) formed particles with comparatively larger diameter than sample T1 (hydrothermal-synthesized MCM-41). However, room temperature synthesis method was preferred due to pore deformation was suspected in sample T1. This was evident in nitrogen isotherm of sample T1, as shown in Fig. 2(a). A pronounced hysteresis loop was found in the isotherm curve. This phenomenon is ascribed by the partial disintegration of pore structure in the sample. Besides, it was found that sample T1 has relatively smaller particle size but lower specific surface area. These results again confirmed that pore structure in sample T1 had deformed and was irregular. Long aging period under high temperature was the main reason of pore deformation. Grün and colleagues also reported similar phenomena in their synthesis of MCM-41 [16].

Table 1
Properties of synthesized MCM-41 (T1 and T2)

Sample	Reaction Condition	Specific Surface Area (m ² /g)	Pore Diameter (nm)	Particle Diameter (nm)
T1	Hydrothermal	683.4	2.79	795
T2	Room Temperature	1138.3	1.99	1016

On the other hand, sample T2 exhibits perfect type IV isotherm for nitrogen sorption curve (Fig. 2(b)). Desorption curve was coincided perfectly on adsorption curve, showing existence of highly regular pore system in particles. A sudden uptake of nitrogen at low pressure (below $p/p^{\circ} = 0.2$)

and a significant reduction in rate of adsorption at high pressure ($p/p^{\circ} > 0.2$) were mainly due to capillary condensation occurred in the mesopores of MCM-41. As pressure increased, majority of the pores in MCM-41 were filled with the condensed liquid, hence, reduced in the rate of adsorption [16]. Formation of MCM-41 with regular pore system will favor gas diffusion during separation process.

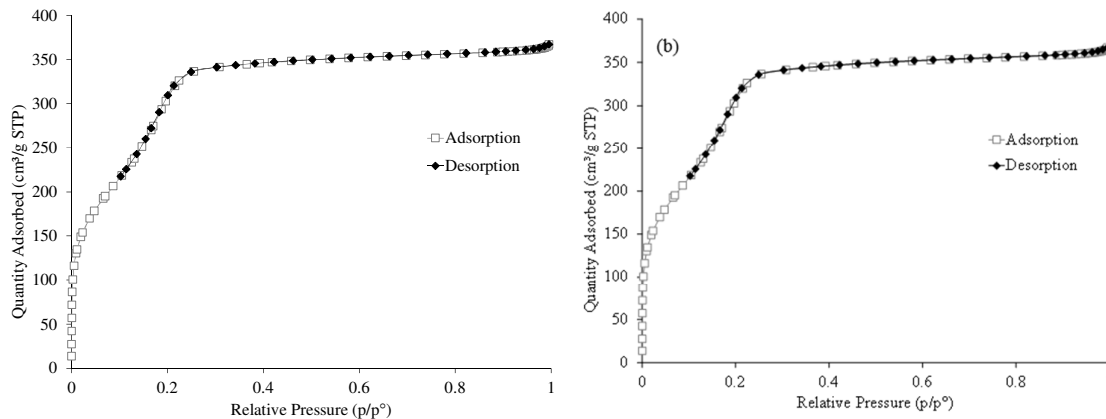


Fig. 2. Nitrogen sorption isotherm of MCM-41 prepared at (a) hydrothermal condition, T1 (b) room temperature, T2

Besides, the hexagonal arrangement of pore system of synthesized MCM-41 was confirmed based on recorded XRD patterns. Figure 3 shows the XRD pattern of synthesized MCM-41. It was noticed that three Bragg peaks appeared at angle between 2° to 6° . Room temperature synthesized MCM-41, sample T2 (Fig. 3(b)), exhibits one high peak at angle 2.87° and two lower intensity peaks at angle 4.79° and 5.39° . These three peaks can be indexed as plane 100, 110 and 200 in hexagonal structure of MCM-41. In addition, the Bragg peaks appear only at low angle of 2 Theta value with no obvious peak above 10° further confirmed the hexagonal arrangement of mesopore structure of MCM-41. The diffraction angles of these peaks also corresponded to the results for MCM-41 in published literature [18-21].

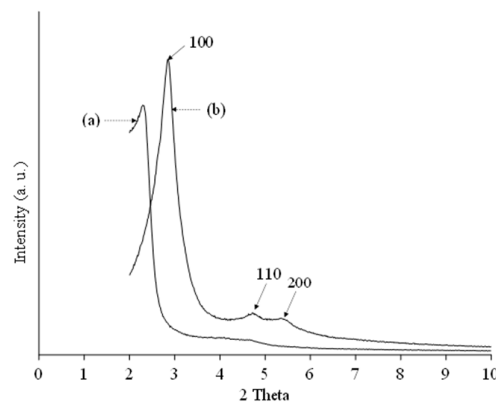


Fig. 3. XRD pattern of synthesized MCM-41 sample (a) T1, (b) T2

By comparing Fig. 3(a) and Fig. 3(b), it can be concluded that MCM-41 prepared under hydrothermal condition (sample T1) has a lower quality of mesopore structure as the peaks indexed as plane 100, 110 and 200 are less defined and shifted to lower 2 Theta value. Shifted peaks are generally attributed by the larger pore diameter of particles. This was evident in average pore diameter calculated using Brunauer Emmett Teller (BET) method (Table 1).

B. Influence of Stirring Rate (250 rpm vs 500 rpm)

Particle size of sample T2 was further reduced by increasing the stirring speed from 250 rpm to 500 rpm. Referring to the properties in Table 2, it was noticed that MCM-41 prepared at stirring rate of 500 rpm (sample T3) formed particles with smaller average diameter compared to sample T2 prepared at lower stirring speed of 250 rpm. Due to smaller particle size, sample T3 was having reasonably greater specific surface area. XRD pattern of sample T3 (Fig. 4(b)) exhibits three peaks at the same angle as sample T2 (Fig. 4(a)) but with high intensity. Increase in peak intensity indicates that a more crystalline structure of MCM-41 was formed [15]. On the other hand, nitrogen sorption isotherm of sample T3 (Fig. 5) exhibits the same type of isotherm (type IV) as sample T2 with no hysteresis phenomena can be seen. These results show that increase of stirring rate does not affect the mesopore structure of particles nevertheless the particles diameter are reduced. The reduction in particles' diameter can be explained through the formation process of particles, known as modified sol-gel process. This process can be divided into two stages: nucleation and growth. During hydrolysis, nucleation happens and starts forming small particles (primary particles) in the solution. The primary particles tend to aggregate and grow into larger secondary particles. In order to prevent aggregation, high speed stirring was introduced in the preparation of small diameter MCM-41.

Table 2
 Properties of synthesized MCM-41 (T2 and T3)

Sample	Diameter (nm)	Stirring Rate (rpm)	Specific Surface Area (m ² /g)	Pore Diameter (nm)	Particle Diameter (nm)
T2		250	1138.3	1.99	1016
T3		500	1325.3	2.17	373

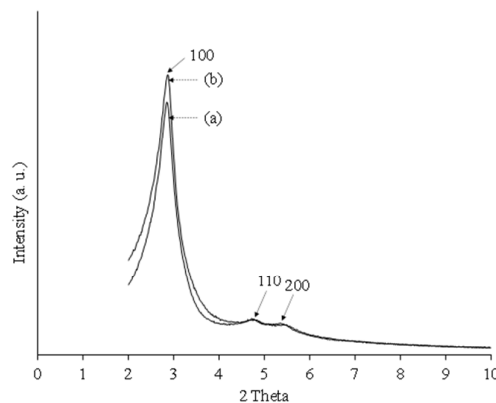


Fig. 4. XRD pattern of synthesized MCM-41 sample (a) T2, (b) T3

Under high stirring rate, primary particles were well-dispersed throughout the solution, hence, growing of particles can be inhibited [10, 22], leading to smaller diameter particles. It was worth-noticed that further increase in stirring rate is not possible due to low volume of synthesis solution used per batch. Furthermore, it was observed that pore diameters of sample T3 was slightly larger than sample T2 which will improve permeability and transport flux of MMM for separation.

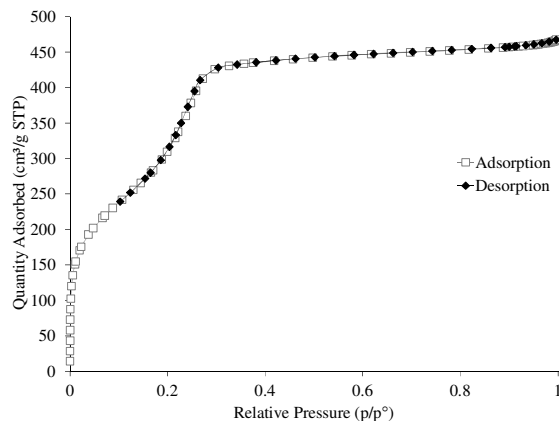


Fig. 5. Nitrogen sorption isotherm of MCM-41 prepared at stirring rate of 500 rpm, T3

C. Types of Post-Synthesis Washing Solution (water + methanol vs methanol only)

In order to reduce the particle size of MCM-41, appropriate washing solution should be used to wash the resultant precipitate. Otherwise, coalescence of particles might occur during the particle drying process which will eventually lead to formation of larger particles or agglomerates. In sample T3, water was used to remove bromide ions from CTAB template. The precipitate was then washed again with methanol in order to remove remaining water. However, it was found that water will have hydrolysis reaction with silicon alkoxide ($\equiv\text{Si-OR}$) and form more silanol groups ($\equiv\text{Si-OH}$). Increase in silanol groups will favor polycondensation reaction to happen in MCM-41 precipitate. Polycondensation reaction will cause also intense aging of particles during precipitate drying process and lead to the formation of larger particles [23]. In order to prevent this, methanol was used instead of water to remove bromide ions. The resultant MCM-41 (sample T4) washed with methanol (Table 3) shows relatively smaller particle diameter (average diameter = 233 nm) compared to sample T3.

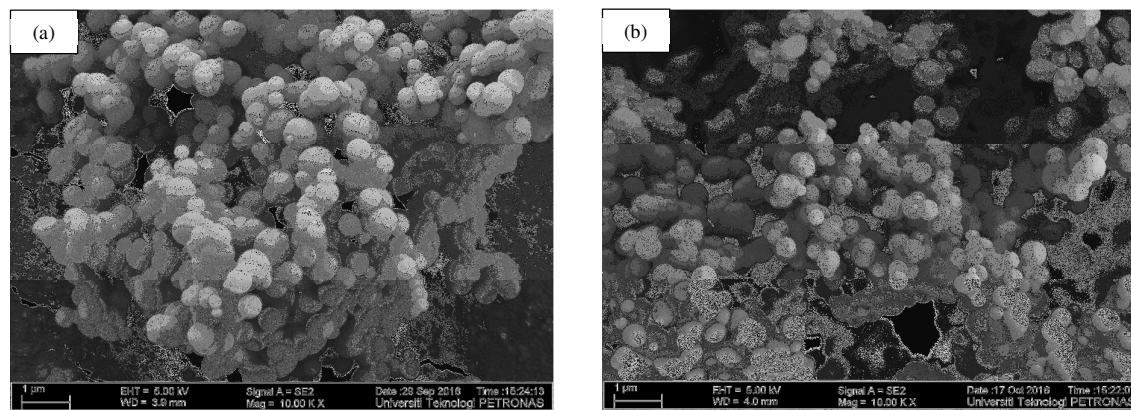


Fig. 6. FESEM image of MCM-41 washed with (a) water + methanol (T3); (b) methanol only (T4)

By referring to Fig. 6, it was also observed that particles size of sample T4 are more even and less agglomerates compared to sample T3. Hence, it can be concluded that washing solution is a critical factor in producing particles with smaller diameter. Furthermore, crystallinity of MCM-41 was further enhanced (showing higher peak intensity) when methanol was used as post-synthesis washing solution (Fig. 7(b)).

Table 3
 Properties of synthesized MCM-41 (T3 and T4)

Sample	Washing Solution	Specific Surface Area (m ² /g)	Pore Diameter (nm)	Particle Diameter (nm)
T3	Water and Methanol	1325.3	2.17	373
T4	Methanol	1367.9	2.17	233

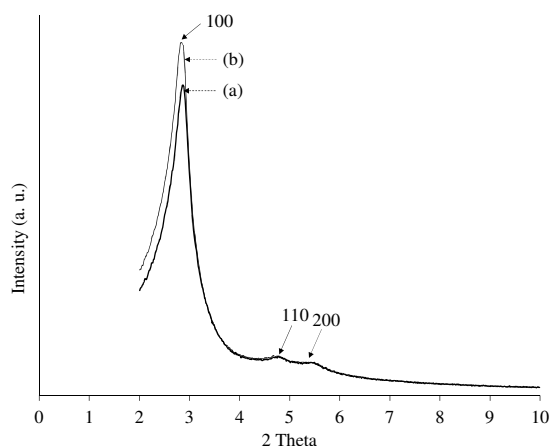


Fig.7. XRD pattern of synthesized MCM-41 sample (a) T3, (b) T4

D. Period of Calcination (5 hours to 20 hours)

Generally, calcination is carried out to remove CTAB surfactant from MCM-41. According to Chen *et al.*, [24] removal of CTAB template was proved successful at a calcination temperature between 550°C to 900°C without collapsing the particles' pores. It was noticed that increased calcination temperature will produce MCM-41 with similar properties. Hence, most of the MCM-41 synthesis was carried out at calcination temperature of 550°C [16, 17, 25]. However, the effect of calcination time towards particles' diameter is still ambiguous. Thus, in this research, MCM-41 was calcined at various period ranging from 5 hours to 20 hours. Referring to Table 4, it was observed that particles' diameter of MCM-41 decreased with increased calcination time up to 15 hours. Reduction in particles' diameter was due to enhancement in intraparticle bonding which causes intraparticle distance to decrease, leading to the formation of smaller particles. This phenomenon was evident in the spacing between planes 100 of the hexagonal structure. Plane 100 spacing reduced with an increased in calcination period. In contrary, samples T5 and T6 undergone short period of calcination demonstrated weaker intraparticle bonds, causing the hexagonal structure of pore systems to be less defined. Low resolution of pore systems arrangement led to broad and

undetectable XRD peaks for planes indexed at 110 and 200 (Fig. 8 (a) and (b)). However, it was noted that particles' diameter increased when resultant MCM-41 (sample T8) was calcined beyond 15 hours. This is because long calcination duration at high temperature will eventually cause crystal boundaries of the particles to enlarge, forming larger particles [26]. Although the particles' diameter were slightly larger, it was detected that the plane 100 spacing of sample T8 was lower compared to sample T7. Both sample T7 and T8 also exhibit similar XRD patterns in which the peaks coincided. Practically, 15 hours of calcination was selected due to shorter synthesis period and smaller resultant particles' diameter was formed.

Table 4
Properties of synthesized MCM-41 (T5, T6, T7 and T8)

Sample	Period of Calcination (hrs)	Spacing d_{100} (nm)	Particle Diameter (nm)
T5	5	3.26	482
T6	10	2.79	472
T4/T7	15	2.58	233
T8	20	2.55	248

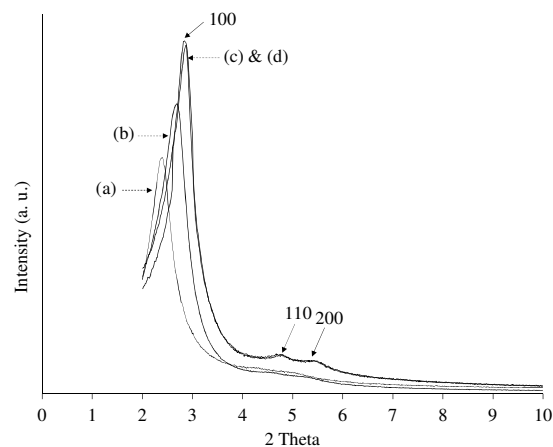


Fig. 8. XRD pattern of synthesized MCM-41 sample (a) T5, (b) T6, (c) T7, (d) T8

In this study, remarkable reduction in particle diameter and increase in specific surface area of MCM-41 were obtained through manipulating various reaction parameters. These interesting results are beneficial towards the advancement of MMM. Particles with smaller diameter or higher specific surface area were proved to have more silanol groups on the surface [27]. Presence of surface silanol groups is a key factor for chemical modification on MCM-41, in which the intention is to enhance the compatibility with polymer and to prevent interface voids or rigidified of polymers that will lead to poor separation. For this reason, the use of small diameter MCM-41 is an advantage in fabrication of MMM for gas separation. In addition, improvement in crystallinity of MCM-41 was also achieved in reduced-size particles. Increase in the degree of crystallinity will consequently enhance selectivity and thermal stability of MMM [23], thus, lower loading of particles is required to be incorporated in MMM in order to achieve the same separation performance.

6. Conclusion

In modified sol-gel process, particle diameter of MCM-41 was found to be sensitive towards several reaction parameters. In order to produce small particle diameter of MCM-41, the synthesis process was suggested to be carried out at room temperature condition and under as high as 500 rpm stirring rate to prevent the formation of secondary particles. Besides, methanol was found to be the appropriate post-synthesis washing solution to remove bromide ions in resultant precipitate. By using methanol as washing solution, hydrolysis reaction between silicon alkoxide and water will be inhibited and preventing polycondensation reaction between silanol groups in precipitate to happen, hence, leading to the formation of smaller diameter MCM-41. Calcined the sample at 550°C for 15 hours was also found to be the optimized period of calcination in order to produce reduced-size MCM-41. Future work may include validation on the effect of particles diameter towards loading, chemical modification and compatibility of MCM-41 with polymer.

Acknowledgement

This research work was supported by Universiti Teknologi PETRONAS and YUTP-FRG, Grant No. 0153AA-E08.

References

- [1] Park, Sunghwan, Joona Bang, Jungkyu Choi, Sang Hyup Lee, Jung-Hyun Lee, and Jong Suk Lee. "3-Dimensionally disordered mesoporous silica (DMS)-containing mixed matrix membranes for CO₂ and non-CO₂ greenhouse gas separations." *Separation and Purification Technology* 136 (2014): 286-295.
- [2] Bushell, Alexandra F., Peter M. Budd, Martin P. Attfield, James TA Jones, Tom Hasell, Andrew I. Cooper, Paola Bernardo, Fabio Bazzarelli, Gabriele Clarizia, and Johannes C. Jansen. "Nanoporous organic polymer/cage composite membranes." *Angewandte Chemie International Edition* 52, no. 4 (2013): 1253-1256.
- [3] He, Xuezhong, and May-Britt Hägg. "Membranes for environmentally friendly energy processes." *Membranes* 2, no. 4 (2012): 706-726.
- [4] Rezakazemi, Mashallah, Abtin Ebadi Amooghin, Mohammad Mehdi Montazer-Rahmati, Ahmad Fauzi Ismail, and Takeshi Matsuura. "State-of-the-art membrane based CO₂ separation using mixed matrix membranes (MMMs): an overview on current status and future directions." *Progress in Polymer Science* 39, no. 5 (2014): 817-861.
- [5] Robeson, Lloyd M. "The upper bound revisited." *Journal of Membrane Science* 320, no. 1-2 (2008): 390-400.
- [6] Jamil, Asif, Oh Pei Ching, and Azmi Shariff. "Current Status and Future Prospect of Polymer-Layered Silicate Mixed-Matrix Membranes for CO₂/CH₄ Separation." *Chemical Engineering & Technology* 39, no. 8 (2016): 1393-1405.
- [7] Kim, Sangil, Liang Chen, J. Karl Johnson, and Eva Marand. "Polysulfone and functionalized carbon nanotube mixed matrix membranes for gas separation: theory and experiment." *Journal of Membrane Science* 294, no. 1-2 (2007): 147-158.
- [8] Dorosti, F., M. R. Omidkhah, M. Z. Pedram, and F. Moghadam. "Fabrication and characterization of polysulfone/polyimide-zeolite mixed matrix membrane for gas separation." *Chemical Engineering Journal* 171, no. 3 (2011): 1469-1476.
- [9] Jomekian, Abolfazl, Majid Pakizeh, Ali Reza Shafiee, and Seyed Ali Akbar Mansoori. "Fabrication or preparation and characterization of new modified MCM-41/PSf nanocomposite membrane coated by PDMS." *Separation and purification technology* 80, no. 3 (2011): 556-565.
- [10] Rahman, Ismail Ab, and Vejayakumaran Padavettan. "Synthesis of silica nanoparticles by sol-gel: size-dependent properties, surface modification, and applications in silica-polymer nanocomposites—a review." *Journal of Nanomaterials* 2012 (2012): 8.
- [11] Klabunde, Kenneth J., Jane Stark, Olga Koper, Cathy Mohs, Dong G. Park, Shawn Decker, Yan Jiang, Isabelle Lagadic, and Dajie Zhang. "Nanocrystals as stoichiometric reagents with unique surface chemistry." *The Journal of Physical Chemistry* 100, no. 30 (1996): 12142-12153.
- [12] Beck, Jeffrey Scott, J. C. Vartuli, W. Jelal Roth, M. E. Leonowicz, C. T. Kresge, K. D. Schmitt, C. T. W. Chu et al. "A new family of mesoporous molecular sieves prepared with liquid crystal templates." *Journal of the American Chemical Society* 114, no. 27 (1992): 10834-10843.

- [13] Reid, Brian D., F. Alberto Ruiz-Trevino, Inga H. Musselman, Kenneth J. Balkus, and John P. Ferraris. "Gas permeability properties of polysulfone membranes containing the mesoporous molecular sieve MCM-41." *Chemistry of materials* 13, no. 7 (2001): 2366-2373.
- [14] Kim, Sangil, and Eva Marand. "High permeability nano-composite membranes based on mesoporous MCM-41 nanoparticles in a polysulfone matrix." *Microporous and Mesoporous Materials* 114, no. 1-3 (2008): 129-136.
- [15] Wu, Hong, Xueqin Li, Yifan Li, Shaofei Wang, Ruili Guo, Zhongyi Jiang, Chan Wu, Qingping Xin, and Xia Lu. "Facilitated transport mixed matrix membranes incorporated with amine functionalized MCM-41 for enhanced gas separation properties." *Journal of Membrane Science* 465 (2014): 78-90.
- [16] Grün, Michael, Klaus K. Unger, Akihiko Matsumoto, and Kazuo Tsutsumi. "Novel pathways for the preparation of mesoporous MCM-41 materials: control of porosity and morphology." *Microporous and mesoporous materials* 27, no. 2-3 (1999): 207-216.
- [17] Teymouri, Mohammad, Abdolraouf Samadi-Maybodi, and Amir Vahid. "A rapid method for the synthesis of highly ordered MCM-41." *International Nano Letters* 1, no. 1 (2011): 34.
- [18] Meléndez-Ortiz, Héctor Iván, Alfonso Mercado-Silva, Luis Alfonso García-Cerda, Griselda Castruita, and Yibrán Argenis Perera-Mercado. "Hydrothermal synthesis of mesoporous silica MCM-41 using commercial sodium silicate." *Journal of the Mexican Chemical Society* 57, no. 2 (2013): 73-79.
- [19] Alahmadi, Sana M., Sharifah Mohamad, and Mohd Jamil Maah. "Synthesis and characterization of mesoporous silica functionalized with calix [4] arene derivatives." *International journal of molecular sciences* 13, no. 10 (2012): 13726-13736
- [20] Ng, Eng-Poh, Jia-Yi Goh, Tau Chuan Ling, and Rino R. Mukti. "Eco-friendly synthesis for MCM-41 nanoporous materials using the non-reacted reagents in mother liquor." *Nanoscale research letters* 8, no. 1 (2013): 120.
- [21] Kruk, Michal, Mietek Jaroniec, Yasuhiro Sakamoto, Osamu Terasaki, Ryong Ryoo, and Chang Hyun Ko. "Determination of pore size and pore wall structure of MCM-41 by using nitrogen adsorption, transmission electron microscopy, and X-ray diffraction." *The Journal of Physical Chemistry B* 104, no. 2 (2000): 292-301.
- [22] Rahman, I. A., P. Vejayakumaran, C. S. Sipaut, J. Ismail, M. Abu Bakar, R. Adnan, and C. K. Chee. "Effect of anion electrolytes on the formation of silica nanoparticles via the sol-gel process." *Ceramics international* 32, no. 6 (2006): 691-699.
- [23] Shin, Jong'Wook, Hyo Jin Kim, Won Ho Jo, Jae Min Hong, B. Jung, and Yong Soo Kang. "Gas Permeation Characteristics in Polyarylate/Poly (butylene terephthalate) Blend Membranes." *Korea Polymer Journal* 3, no. 2 (1995): 65-70.
- [24] Chen, Cong-Yan, Hong-Xin Li, and Mark E. Davis. "Studies on mesoporous materials: I. Synthesis and characterization of MCM-41." *Microporous materials* 2, no. 1 (1993): 17-26.
- [25] Voegtlin, A. C., A. Matijasic, J. Patarin, C. Sauerland, Y. Grillet, and L. Huve. "Room-temperature synthesis of silicate mesoporous MCM-41-type materials: influence of the synthesis pH on the porosity of the materials obtained." *Microporous materials* 10, no. 1-3 (1997): 137-147.
- [26] Pawar, Bharat G., Dipak V. Pinjari, Sanjay S. Kolekar, Aniruddha B. Pandit, and Sung H. Han. "Effect of Sintering Temperatures on the Synthesis of S n O 2 Nanospheres." *ISRN Chemical Engineering* 2012 (2012).
- [27] C. J. Brinker and G. W. Scherer, Sol-Gel Science. USA: Academic Press, 1990, pp. 617-668.